CHEMISTRY
A EUROPEAN JOURNAL

DOI: 10.1002/chem.200801851

# Mono- and Bis(tetrathiafulvalene)-1,3,5-Triazines as Covalently Linked Donor–Acceptor Systems: Structural, Spectroscopic, and Theoretical Investigations

**François Riobé,[a] Philippe Grosshans,[b] Helena Sidorenkova,[b] Michel Geoffroy,*[b] and Narcis Avarvari*[a]**

**Abstract:** Reaction of 2,4,6-trichloro-1,3,5-triazine with lithiated tetrathiafulvalene (TTF) in stoichiometric conditions, followed by treatment with sodium methanolate, provides mono- and bis(TTF)–triazines as new covalently linked (multi)donor–acceptor systems. Single-crystal X-ray analyses reveal planar structures for both compounds, with formation of peculiar segregated donor and acceptor stacks for the mono(TTF)–triazine compound, while mixed TTF–triazine stacks establish in the case of the bis(TTF) derivative. Cyclic voltammetry measurements show reversible oxidation of the TTF units, at rather low potential, with no splitting of the oxidation waves in the case of the dimeric TTF, whereas irreversible reduction of the triazine core is observed. Intramolecular charge transfer is experimentally evidenced through solution electronic absorption spectroscopy. Time-dependent DFT calculations allow the assignment of the charge transfer band to singlet transitions from the HOMO of the donor(s) to the LUMO of the acceptor. Solution EPR measurements correlated with theoretical calculations were performed in order to characterize the oxidized species. In both cases the spectra show very stable radical species and contain a triplet of doublet pattern, in agreement with the coupling of the unpaired electron with the three TTF protons. The dication of the bis(TTF)–triazine is paramagnetic, but no spin–spin exchange interaction could be detected.

**Keywords:** charge transfer · donor–acceptor systems · EPR spectroscopy · nitrogen heterocycles · structure elucidation · tetrathiafulvalenes

## Introduction

Covalently linked donor–acceptor (D–A) dyads in which the donor unit is a tetrathiafulvalene (TTF) derivative[1] are a well-known class of precursors for molecular metals and superconductors.[2] They have received much attention especially in the last few years because of their potential applications in molecular electronics and optoelectronics, photovoltaics, nonlinear optics,[1a,3] although the use of bridged D(TTF)–σ-A(TCNQ) (TCNQ = tetracyano-*p*-quinodimethane) dyads as molecular rectifiers was theoretically postulated in 1974.[4] Undoubtedly, the important feature in such compounds is the possibility for an intramolecular charge transfer (ICT) to occur; this clearly depends on the nature of the linkage between the redox active units. The systems characterized so far consist either of fused TTF–acceptor derivatives, with acceptor moieties such as dipyridophenazine,[5] diquinone,[6] pyrazine,[7] and phtalocyanine,[8] or in compounds containing a σ-type spacer between the TTF unit and acceptors like TCNQ,[9] tetracyanoanthraquinodimethane (TCNAQ),[10] $C_{60}$,[11] carbon nanotubes,[12] fluorene,[13] $TCNQF_4$,[14] and pyridinium cations,[3a,15] or a π-conjugated spacer such as a double bond between the TTF and a pyridinium cation,[16] or a triple bond between the TTF and pyridine[17] or 2,2′-bipyridine units.[18] However, only a few TTF–A compounds described so far have a direct link

[a] F. Riobé, Dr. N. Avarvari
Université d'Angers, CNRS
Laboratoire de Chimie et Ingénierie Moléculaire
CIMA UMR 6200, UFR Sciences, Bât. K
2 Bd. Lavoisier, 49045 Angers (France)
Fax: (+33) 02-41-73-54-05
E-mail: narcis.avarvari@univ-angers.fr

[b] Dr. P. Grosshans, Dr. H. Sidorenkova, Prof. M. Geoffroy
Department of Physical Chemistry, University of Geneva
30 Quai Ernest Ansermet, 1211 Geneva (Switzerland)
Fax: (+41) 22-379-6103
E-mail: Michel.Geoffroy@chiphy.unige.ch

Supporting information for this article is available on the WWW under http://dx.doi.org/10.1002/chem.200801851.

between the TTF unit and the acceptor, such as in TTF–pyridinium cations,[19] or an oxophenalenoxyl–TTF derivative,[20] thus leading to a more efficient intramolecular charge transfer and to planar structures, as a consequence of the conjugation between the donor and acceptor. In this respect this type of derivative can be compared with the fused TTF–acceptor systems that also posses these advantages. Note that an extensive series of TTF–pyridine, –pyrimidine and –quinoline derivatives, as redox active ligands precursors for multifunctional materials in which the TTF was directly connected to the nitrogen heterocycles, have been reported, but without any mention though to a possible ICT.[21] A particularly interesting acceptor unit is represented by the 1,3,5-triazine skeleton, which, besides its electron-acceptor character, possesses luminescence properties in certain derivatives,[22] and, moreover, substituted triazines can be sequentially synthesized starting from the commercially available 2,4,6-trichloro-1,3,5-triazine (cyanuric chloride) reagent. Nevertheless, to our knowledge, only a single example of covalently linked TTF–triazine derivative has been mentioned to date,[23] without structural characterization though, nor further investigations. We report herein the synthesis and structural characterization of unprecedented planar D–A systems consisting in directly linked mono- (**1**) and bis-(TTF)–1,3,5-triazines (**2**), together with experimental and theoretical evidence for intramolecular charge transfer. We also report on solution EPR measurements of the radical cation species of both compounds, in order to account for the electron delocalization, correlated with theoretical calculations.

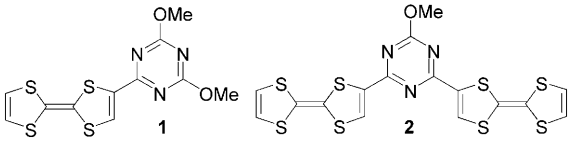


## Results and Discussion

**Synthesis and solid-state structures**: The TTF–dimethoxy-1,3,5-triazine **1** and bis(TTF)–methoxy-1,3,5-triazine **2** were synthesized by nucleophilic substitution of one or two chlorine atoms by TTF units upon reaction between lithiated TTF and 2,4,6-trichloro-1,3,5-triazine, followed by quenching in situ the intermediate TTF–dichloro-1,3,5-triazine and bis-(TTF)–chloro-1,3,5-triazine with sodium methanolate to replace the remaining chlorine substituents by methoxy groups (Scheme 1).

Conversely, methoxydichlorotriazine can be also used as reagent towards lithiated TTF, to obtain **1** with higher yields.[24] Note that a small amount of the $C_3$-symmetric tris-(TTF)–triazine, as confirmed by mass spectrometry,[24] was also isolated, yet its complete lack of solubility precluded any structural investigations. The D–A compound **1**, obtained as dark red crystals upon recrystallization in acetonitrile, crystallizes in the monoclinic system, space group

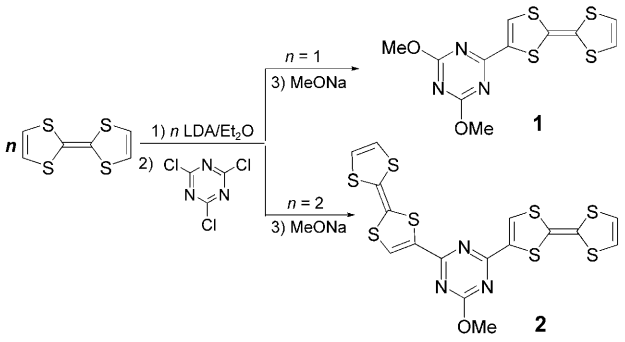


Scheme 1. Synthetic procedure for **1** and **2**.

$P2_1/c$.[24] Interestingly, the overall geometry of the molecule is close to planarity, as shown by the small value of only 6.14° for the dihedral angle between the adjacent dithiole and triazine mean planes, thus indicating a certain degree of conjugation between the donor and acceptor. Moreover, short N1···S1 intramolecular contacts of 2.91 Å are observed, which probably favor the mutual planarization of the donor and acceptor moieties, besides the likely conjugation in between thanks to the direct linkage (Figure 1).

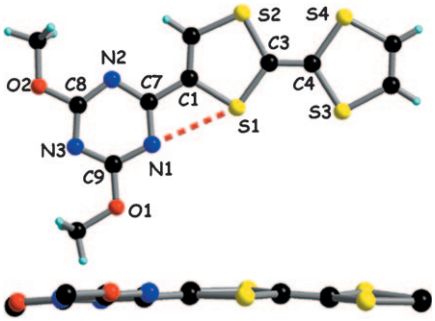


Figure 1. Molecular structure of **1**, along with a side view of the molecule.

The packing diagram shows a complete segregation of donor and acceptor fragments, which organize in homostacks of TTF and triazine along *b* in a head-to-head alignment, with rather short intra- and interstack S···S contacts, within 4 Å, as emphasized in Figure 2. This peculiar architecture is an important prerequisite in view of the design of electronic devices such as TTF-based field-effect transistors.[25]

Compound **2**, containing two donor TTF moieties covalently linked to one acceptor triazine molecule, crystallizes as violet plates in the monoclinic system, space group *C*2/*c*. Once again, the molecule shows almost planar conformation in the solid state, with small values of 8.61° and 6.65° for the two characteristic dihedral angles between the triazine ring and the mean planes of the adjacent dithiole rings S1A–S2A and S1B–S2B, respectively. Also, as previously observed in the structure of **1**, short intramolecular N···S contacts amounting to 2.87–2.88 Å are established (Figure 3).

  

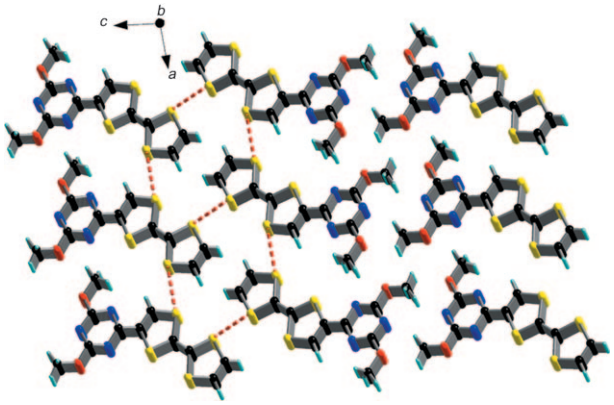


Figure 2. Packing diagram of **1** along *b*, with an emphasis on short interstack S···S contacts (3.49–3.57 Å).

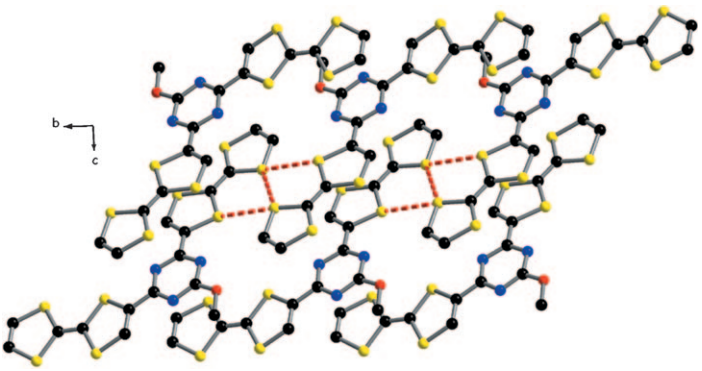


Figure 4. Packing diagram of **2** along *a*, with an emphasis on short S···S contacts (3.52–3.56 Å). H atoms have been omitted.

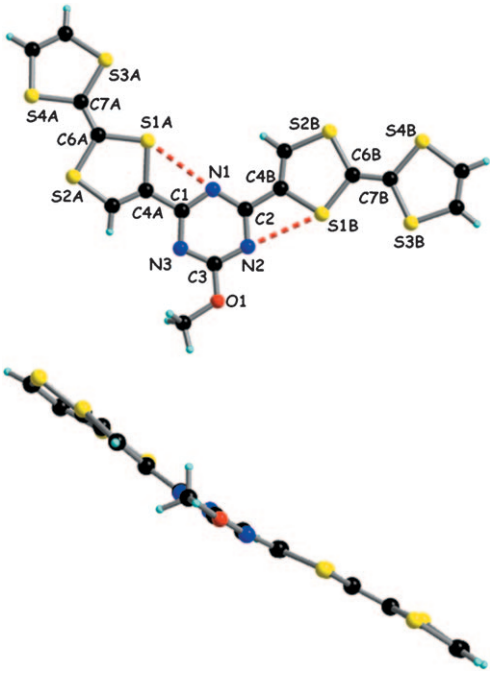


Figure 3. Molecular structure of **2**, along with a side view of the molecule.

However, unlike the previous D–A system, there is no segregation this time between the donor and acceptor parts in the packing at the solid state; the molecules stack upon formation of D–A–D triads, with rather short intermolecular D···A distances of around 3.5–3.6 Å (Figure 4). Lateral intermolecular S···S contacts as short as 3.52 Å are observed in the *bc* plane, while the shortest S···S distances along the stacking direction *a* are at the van der Waals limit.

Cyclic voltammetry measurements demonstrate good donor ability for both compounds, with reversible oxidations at +0.41 V and +0.79 V versus SCE for **1**, and +0.43 V and 0.76 V versus SCE for **2**.[24] The values of the first oxidation potentials are slightly anodically shifted when compared to the parent TTF.[1] Note the somewhat broader signals in the case of **2**, a likely consequence of two successive one-electron oxidation processes. In the region of negative potentials one can observe the irreversible reduction of the triazine unit, at −1.98 V and −1.65 V for **1** and **2**, respectively, in agreement with its electron-acceptor character.[26] There is evidently a quite large difference between the reduction potentials of **1** and **2**, suggesting a stronger electron-acceptor character for the triazine in the latter.

**UV/Vis spectroscopy and theoretical calculations**: To evidence the occurrence of donor-to-acceptor ICT, solution UV/Vis/NIR measurements were performed (Figure 5). In

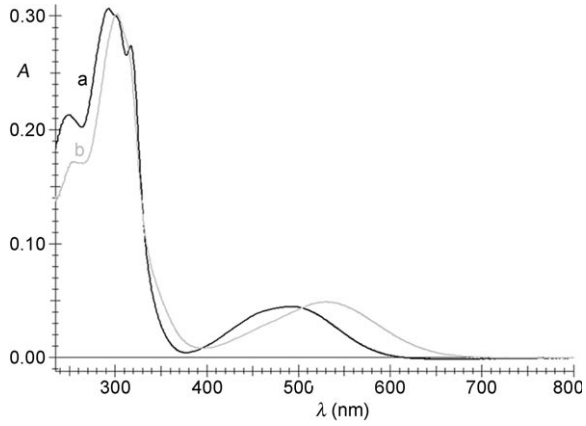


Figure 5. UV/Vis spectra of a) **1** ($\lambda_{max}$ = 492 nm, $\varepsilon$ = 2251 L mol$^{-1}$ cm$^{-1}$, $c$ = $2\times10^{-5}$ M) and b) **2** ($\lambda_{max}$ = 530 nm, $\varepsilon$ = 6960 L mol$^{-1}$ cm$^{-1}$, $c$ = $7.2\times10^{-6}$ M).

the absorption spectra of both compounds, besides the typical TTF absorption band centered around 300 nm, broad bands in the visible region at $\lambda_{max}$ 492 nm for **1** and 530 nm for **2**, characteristic of ICT,[5a] can be observed and they are clearly responsible for the dark red or violet colors of our compounds. The difference between the $\lambda_{max}$ of the two bands indicates a smaller HOMO–LUMO gap for **2**, also in agreement with the CV measurements. Note that a charge-transfer band is not observed in a solution prepared from TTF and a methoxytriazine derivative,[24] thus ruling out the hypothesis of an intermolecular charge transfer.

  

Usually, theoretical calculations allow the assignment of these bands to $HOMO_D \rightarrow LUMO_A$ electronic transitions. To have a better understanding on the nature of the D–A character of our compounds, we performed theoretical calculations at DFT/B3LYP/6-31+G* level on the neutral **1** and **2**, starting from the experimental X-ray structures as input geometries. Accordingly, DFT optimization on **1** leads to four energy minima (only positive frequencies) corresponding to practically planar conformations of $C_1$ symmetry, with very small dihedral angles between the triazine and the adjacent dithiole ring amounting to 1° and differing in between by the relative orientation of the methoxy groups.[24] The four equilibrium geometries have essentially the same energy ($\Delta E_{max-min} = 1.05$ kcal mol$^{-1}$) and one of them, which is only 0.45 kcal mol$^{-1}$ above the global minimum, corresponds to the orientation of the methoxy groups observed in the solid state. We therefore analyzed the frontier orbitals on this conformation. As can be observed in Figure 6 the HOMO is

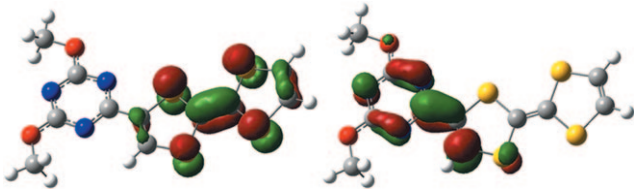

Figure 6. HOMO (left) and LUMO (right) of **1** (DFT/B3LYP/6-31+G*).

of π-TTF type, while the LUMO, also of π-type and rather low in energy (−2.103 eV), is mainly based on the triazine unit, yet with a sizeable participation of the dithiole half directly linked to the triazine. This last feature indicates a certain degree of conjugation between the donor and acceptor units. The associated HOMO–LUMO energy gap amounts to 2.75 eV.

DFT optimization for **2** also leads to four energy minima which are practically isoenergetic ($\Delta E_{max-min} = 0.84$ kcal mol$^{-1}$), with the corresponding conformations of $C_1$ symmetry being practically planar, as demonstrated by the small values of about 1° for the dihedral angles between the triazine ring and the adjacent dithiole halves.[24] The differences between the four equilibrium geometries rely on the relative orientation of the TTF units and the methoxy group, one of them corresponding to the experimental solid-state structure. Accordingly we based our orbital analysis on this conformation (Figure 7). The HOMO and HOMO−1, both of π type, are developed respectively on each TTF unit, with an energy difference in between of 104 meV. The LUMO, even lower in energy (−2.429 eV) when compared to the LUMO of **1**, extends mainly over the triazine unit, but also on both adjacent dithiole halves, thus suggesting a conjugation in the molecule and an enhanced electron-acceptor character (Figure 7). The HOMO–LUMO energy gap is now 2.42 eV, in agreement with the observation of the ICT band at higher wavelength in the UV/Vis spectrum. The calculations also correlate with the cyclic voltammetry measurements (vide supra).

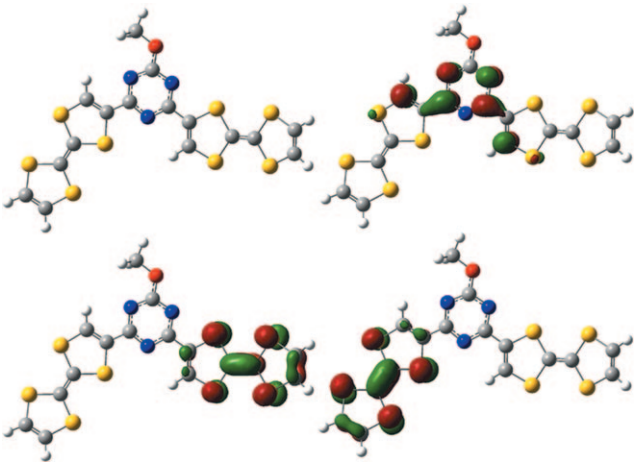

Figure 7. Optimized geometry (top left) and LUMO (top right) and HOMO and HOMO−1 (bottom left and right) for **2** (DFT/B3LYP/6-31+G*).

Furthermore, vertical excitations were calculated on the optimized ground state geometry of **1** and **2**, at the time-dependent DFT level.[24] For **1**, the lowest energy allowed singlet transition, predicted to be at 2.31 eV (536 nm), with an oscillation strength $f = 0.067$, is of $\pi_{HOMO}$–$\pi^*_{LUMO}$ type, clearly corresponding to an intramolecular CT transition from the TTF donor to the triazine acceptor. Moreover, the theoretical value for the transition energy is in excellent agreement with the experimental one deduced from the UV/Vis spectrum. On the other hand, since in **2** HOMO and HOMO−1 are relatively close in energy and possess the same symmetry, the lowest energy transition, calculated at 2.04 eV (608 nm) with an oscillation strength $f = 0.144$, appears as a combination of ICT from both TTF donors towards the LUMO of the triazine. Once again, the calculated transition energy, which is red-shifted when compared to **1**, correlates with the experimental value.

**EPR spectroscopy and theoretical calculations**: One of the main objectives in the TTF field relies on the preparation of radical cation salts upon chemical or electrochemical oxidation. We therefore decided to characterize the oxidized species of **1** and **2** in solution by the means of EPR spectroscopy to have a quantitative estimation of the electron delocalization in these radicals. In particularly, one important question to address concerns the nature of the dication $\mathbf{2}^{2+}$, that is, diamagnetic or paramagnetic species, taking into account that both TTF units in **2** are likely to oxidize at the same potential when considering the unique oxidation wave observed in cyclic voltammetry (vide supra). In this respect, the study of the radical cation $\mathbf{1}^{\bullet+}$ would provide us first helpful information about electronic distribution in a mono-(TTF)–triazine system, which could be then compared with those obtained in the case of the bis(TTF)–triazine compound. Electrochemical oxidation of a solution of **1** in THF,

  

in situ in the EPR cavity, leads to an intense EPR spectrum centered at $g=2.0083$. As shown in Figure 8, the hyperfine structure results from the coupling with three spin $^1/_2$ nuclei:

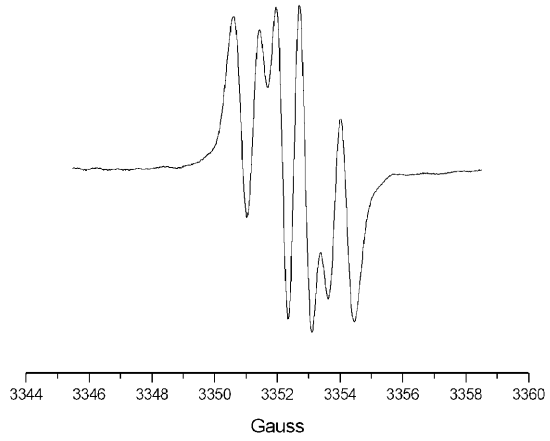


Figure 8. EPR spectrum observed by electrochemical oxidation of **1**.

two protons with a coupling constant $A_{iso}=3.6$ MHz and an additional proton with $A_{iso}=2.2$ MHz. The shape of the lines suggests that some unresolved hyperfine couplings and motion effects cause a broadening of the signals.

The corresponding radical species is very stable and, at room temperature, its spectrum is observed several hours after the voltage has been switched off. The same spectrum is obtained by chemical oxidation of a solution of **1** with the ferricinium salt $[Cp_2Fe][PF_6]$. It is worthwhile mentioning that chemical oxidation can lead to some aggregation/flocculation which can cause an appreciable broadening of the EPR signals; it is therefore important to work with much diluted solutions ($10^{-6}$ M). To rationalize the EPR results, we performed unrestricted DFT calculations on the radical cation species of **1**. First, geometry optimization on $\mathbf{1}^{\bullet+}$ afforded, as in the case of the neutral precursor, four energy minima,[24] which are now perfectly planar, that is, $C_s$ symmetric, and very close in energy within an energy range of $\Delta E_{max-min}=4.47$ kcal mol$^{-1}$, corresponding to the four possible orientations of the methoxy groups. The optimized geometry and SOMO for the global minimum are represented in Figure 9.

Consistent with the SOMO, calculation of the spin densities, ranging between 16 and 19% for the S atoms and amounting to 10 and 12% for the central C6 and C10 atoms, respectively, clearly indicates that the unpaired electron is totally localized on the TTF moiety. The resulting hyperfine coupling constants, calculated at the DFT/B3LYP/aug-cc-pPVDZ level,[24] reproduce the triplet of doublets observed on the EPR spectrum very well, since the two protons, H13 and H14 bound to C11 and C12, respectively, present the same coupling constant $A_{iso}=-3$ MHz, while the proton H9 attached to C7 is characterized by a smaller constant $A_{iso}=-2$ MHz. All other coupling constants are very small (averaged $A_{iso}=0.07$ MHz for $^1$H for the methyl

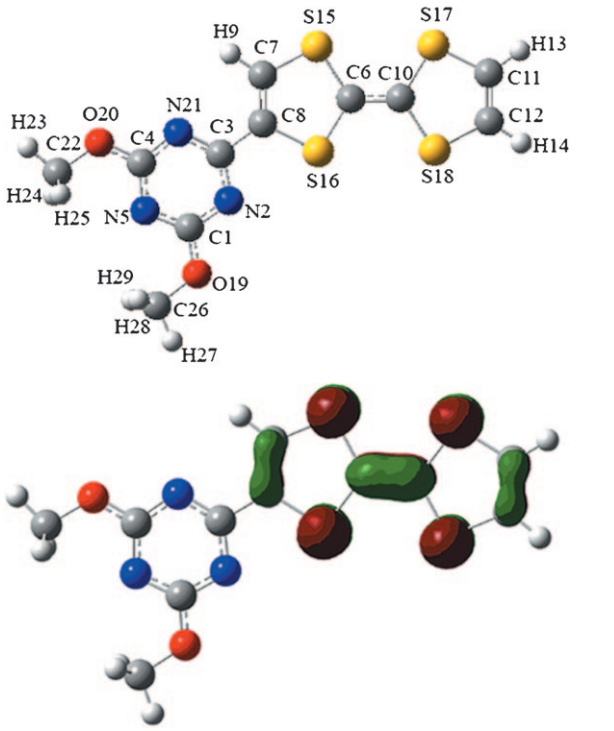


Figure 9. Optimized geometry with atom labeling and SOMO for $\mathbf{1}^{\bullet+}$ (DFT/B3LYP/6-31+G*).

group C22; and $A_{iso}=0.64$, 0.65, $-0.18$ MHz for $^{14}$N for N21, N5, N2, respectively) and, likely, contribute only to a broadening of the EPR lines. Clearly, cyclic voltammetry, EPR measurements and DFT calculations show that oxidation of **1** leads to a very stable radical cation mainly localized on the TTF moiety.

Cyclic voltammetry measurements (vide supra) in the case of the compound **2** suggest undoubtedly that formation of the dication species is very likely favored upon oxidation. Similar bis(TTF) donors described by Iyoda et al.,[27] containing a benzene or a pyridine spacer between the redox active units located in *meta* position with respect to each other on the aromatic rings, also shown a pair of two-electron oxidation waves at comparable potential values. It was postulated on the basis of a spin-polarization mechanism that the dication species should have a triplet ground state due to ferromagnetic coupling between the two TTF radical cations. Theoretical calculations at unrestricted Hartree–Fock level for 1,3-bis(TTF)benzene also predict that the triplet state is more stable than the singlet.[28] However, to our knowledge, these assumptions have not been experimentally proved. Note that EPR investigations evidenced spin–spin exchange interactions within a series of biradical dications of dimeric TTFs containing 1,1-vinyl linkers.[29] In the present study, electrolysis of a solution of the bis(TTF)–triazine **2** in THF, at a potential corresponding to the first oxidation wave, gave rise to oxidized species for which the EPR spectrum resembles to the one obtained for $\mathbf{1}^{\bullet+}$, since it also contains a triplet of doublet pattern (Figure 10).

  

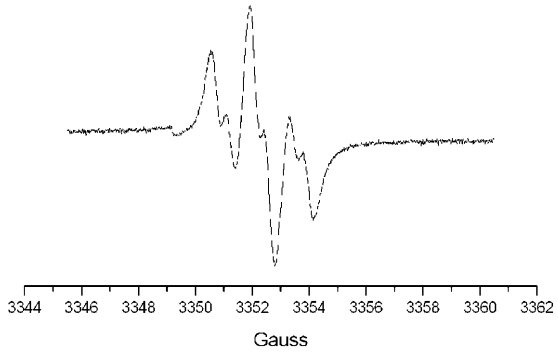


Figure 10. EPR spectrum observed by electrochemical oxidation of **2**.

Both coupling constants slightly differ when compared to those measured in the case of **1**. Indeed, the coupling constant with two equivalent protons, thus accounting for the triplet, amounts to 3.9 G, whereas a constant of 1.2 G is measured for the third proton. A large increase of the voltage does not alter this spectrum which is particularly persistent. Clearly, this spectrum is not due to a radical species delocalized over the entire molecule. To clarify the nature of the oxidation product, several experiments were carried out by using $[Cp_2Fe]PF_6$ as oxidizing agent and by varying the ratio $\rho = [\text{oxidant}]/[\mathbf{2}]$ ($\rho = 0.25$, 0.5, 1, 2) in such a way that a couple of samples very likely contain a mixture of neutral, monocationic, and dicationic species in equilibrium, with probably the monocation in larger amount than the dication ($\rho = 0.25$ and 0.5), while the sample with $\rho = 2$ essentially contains only the dication. All measurements were carried out at very low concentration to avoid any aggregation or precipitation. Except for their intensity, which increased with $\rho$, all spectra were identical to the one shown in Figure 10. This suggests that both the monocation and the dication of **2** lead to the same spectrum, which exhibits coupling constants close to those observed for the radical monocation $\mathbf{1}^{\bullet+}$ containing a single TTF unit. As explained in pioneer investigations of Rassat et al. with biradicals containing two nitroxide groups,[30] and exemplified later on in other biradical compounds,[31] the mono- and biradicals have the same coupling constants when the spin exchange coupling constant $J$ is small compared to the hyperfine coupling. This implies $J$ close to zero for $\mathbf{2}^{2+}$ and, therefore, one can conclude that the triazine ring makes the two TTF units practically independent.

Furthermore, DFT calculations were performed on the dication $\mathbf{2}^{2+}$ for its triplet state. Accordingly, geometry optimization afforded four minima of $C_s$ symmetry within an energy range $\Delta E_{max-min} = 2.83\ \text{kcal mol}^{-1}$, corresponding to different relative orientations of the methoxy group and the TTF units.[24] As expected, there is a degeneracy at the HOMO level, with the two π-type orbitals located on each TTF respectively, while the global minimum corresponds to a $C_2$ symmetric conformation if one does not take into account the methoxy group which breaks this symmetry (Figure 11).

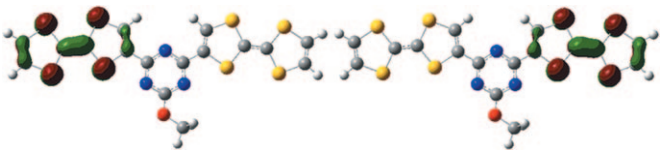

Figure 11. HOMO and HOMO−1 for $\mathbf{2}^{2+}$ (DFT/B3LYP/6-31+G*).

The calculated coupling constants (DFT/B3LYP/aug-cc-pPVDZ) are the same for the four minima and amount to $A_{iso} = -2$ MHz for the coupling with the external TTF protons and to $A_{iso} = -1$ MHz for the coupling with the internal TTF protons. Consistent with the experimental spectrum, for $J = 0$, these values lead to an hyperfine structure composed of a triplet of doublet. Clearly the dication $\mathbf{2}^{2+}$ is paramagnetic, yet with no sizeable exchange interactions between the unpaired electrons of each TTF.

## Conclusion

During this work, covalently linked donor–acceptor systems based on the unprecedented direct linkage between one or two TTF donors and a 1,3,5-triazine unit have been synthesized through a simple synthetic procedure. Interestingly, single-crystal X-ray analyses revealed planar structures, with formation of segregated column of TTF donors and triazine acceptors in the case of the TTF–triazine **1**, and establishment of mixed donor-acceptor stacks in the packing of the (bis)TTF–triazine **2**. Intramolecular charge transfer (ICT), arising from HOMO–LUMO singlet transitions, has been experimentally evidenced through solution UV/Vis spectroscopy and theoretically confirmed by time-dependent DFT calculations. The extent of the electron delocalization in the radical cation $\mathbf{1}^{\bullet+}$ and in the dication $\mathbf{2}^{2+}$, generated upon chemical or electrochemical oxidation of the precursors, has been investigated by EPR spectroscopy and theoretical calculations. Thus, both donor–acceptor derivatives we described here are certainly interesting molecular materials precursors in view of their solid-state structures and electronic properties. Further studies concerning especially photophysical investigations, as well as the synthesis of soluble $C_3$ symmetric tri(TTF)–triazine derivatives are under active investigation in our laboratories.

## Experimental Section

**General**: Dry $CH_2Cl_2$ and $CH_3CN$ were obtained by distillation over $P_2O_5$ and THF and diethyl ether were distilled over sodium and benzophenone. NMR spectra were recorded on a Bruker Avance DRX500 spectrometer operating at 500.04 MHz for $^1H$. Chemical shifts are expressed in parts per million (ppm) downfield from external TMS. The following abbreviations are used: s, singlet; d, doublet. The EI MS spectrum of **1** was recorded on a Thermo Electron Corporation TRACE-DSQ apparatus, with direct introduction probe at 70 eV, while the MALDI-TOF MS spectrum of **2** was recorded on Bruker Biflex-IIITM apparatus,

  

equipped with a 337 nm $N_2$ laser. Elemental analyses were performed by the "Service d'Analyse du CNRS" at Gif/Yvette, France.

**Method A for 1 and 2**: LDA (2.4 mmol, 1.2 mL, 2 M in hexanes) was added to a solution of tetrathiafulvalene (TTF) (409 mg, 2 mmol) in diethyl ether (15 mL) at −78 °C under magnetic stirring. The mixture was stirred for 45 min and a yellow precipitate appeared. Then a solution of cyanuric chloride (74 mg, 0.4 mmol, 0.2 equiv) in THF (30 mL) was added dropwise. The color turned immediately to blue, and then to black when the solution was allowed to warm at RT. Then, MeONa (65 mg, 1.2 mmol) in methanol (10 mL) was added and the color slowly changed to red. The mixture was filtered onto celite, concentrated under vacuum and chromatographed. Two main products **1** (red powder) and **2** (purple powder) could be separated on silica gel (DCM:cyclohexane 1:1 as eluant), with the later eluted first. Most of the unreacted TTF could be also recovered by chromatography. A very small amount of the $C_3$-symmetric tris(TTF)–triazine derivative was also isolated with this procedure.[24]

**2-Tetrathiafulvalene-4,6-dimethoxy-1,3,5-triazine (1)**: Yield: 20 mg (3%); $^1$H NMR ($CDCl_3$): $\delta = 4.06$ (s, 6H; C*H*$_3$O), 6.32 (d, $^3J_{HH} = 6.2$ Hz, 1H; C*H*=CH), 6.34 (d, $^3J_{HH} = 6.2$ Hz, 1H; CH=C*H*), 7.81 ppm (s, 1H; C*H*=C-C=N); $^{13}$C NMR ($CDCl_3$): $\delta = 55.4$, 108.3, 113.2, 118.7, 119.3, 134.9, 167.8, 172.3 ppm; MS (EI$^+$-DSQ): $m/z$: 342.96 ($M_{th} = 342.96$); elemental analysis calcd (%) for $C_{11}H_9N_3O_2S_4$: C 38.47, H 2.64, N 12.23; found: C 38.71, H 2.44, N 11.97.

**2,4-Bis(tetrathiafulvalene)-6-methoxy-1,3,5-triazine (2)**: Yield: 10 mg (3%); $^1$H NMR ([D$_8$]THF): $\delta = 4.06$ (s, 3H; C*H*$_3$O), 6.54 (d, $^3J_{HH} = 6.2$ Hz, 1H; C*H*=CH), 6.57 (d, $^3J_{HH} = 6.2$ Hz, 1H; CH=C*H*), 8.07 (s, 2H; C*H*=C-C=N); MS (MALDI-TOF): $m/z$: 514.84 ($M_{th} = 514.85$); elemental analysis calcd (%) for $C_{16}H_9N_3OS_8$ : C 37.26, H 1.76, N 8.15; found: C 36.91, H 1.95, N 8.01. Unfortunately, because of the sparing solubility of **2** in all deuterated solvents, including [D$_8$]THF, we were not able to record a $^{13}$C NMR spectrum.

**Method B for 2**: LDA (1.65 mmol) freshly prepared (0.23 mL of diisopropylamine and 1 mL of BuLi (1,6 M in hexanes) in diethyl ether (10 mL) were added to a solution of TTF (306 mg, 1.5 mmol) in $Et_2O$ (15 mL) at −78 °C. After one hour, a solution of cyanuric chloride (69 mg, 0.38 mmol) in THF (50 mL) was added dropwise. Then, the mixture was allowed to warm slowly (5 h). At −15 °C, MeONa (30 mg, 0.57 mmol) in methanol (15 mL) was added and the color turned to purple. The mixture was treated at RT as previously to obtain **2** (80 mg, 21%).

**Method C for 1**: 2,4-Dichloro-6-methoxy-1,3,5-triazine (180 mg, 1 mmol) in THF (50 mL) was added to a solution of lithium-tetrathiafulvalene (1 mmol), prepared in situ as in method B, in diethyl ether (15 mL) at −78 °C. The mixture was allowed to warm to −10 °C. Then, MeONa (108 mg, 2 mmol) in methanol (15 mL) was added. The color turned immediately to red. After one night at RT, the mixture was filtered onto celite, concentrated under vacuum and the resulting mixture purified by chromatography on silica gel (DCM:cyclohexane 1:1) to afford **1** as a red powder (37 mg, 11%).

**X-ray structure determinations**: Details about data collection and solution refinement are given in Table 1. X-ray diffraction measurements were performed on a Bruker Kappa CCD diffractometer, operating with a $Mo_{K\alpha}$ ($\lambda = 0.71073$ Å) X-ray tube with a graphite monochromator. The structures were solved (SHELXS-97) by direct methods and refined (SHELXL-97) by full-matrix least-square procedures on $F^2$.[32] All non-hydrogen atoms were refined anisotropically, apart from the C7 carbon atom in **1**. Hydrogen atoms were introduced at calculated positions (riding model), included in structure factor calculations but not refined. Crystals of **1** were very thin needles, therefore the data set was only of medium quality.

**Electrochemical studies**: Cyclic voltammetry measurements were performed in a glove box containing dry, oxygen-free (<1 ppm) argon, by using a three-electrode cell equipped with a platinum millielectrode of 0.126 cm$^2$ area, an Ag/Ag$^+$ pseudo-reference electrode and a platinum-wire counter electrode. The potential values were then re-adjusted with respect to the saturated calomel electrode (SCE). The electrolytic media involved a 0.1 mol L$^{-1}$ solution of ($n$-Bu$_4$N)PF$_6$ in THF. All experiments were performed at room temperature at 0.1 V s$^{-1}$. Experiments were carried out with an EGG PAR 273 A potentiostat with positive feedback compensation.

Table 1. Crystallographic data, details of data collection and structure refinement parameters.

| | **1** | **2** |
|---|---|---|
| formula | $C_{11}H_9N_3O_2S_4$ | $C_{16}H_9N_3OS_8$ |
| $M$ [g mol$^{-1}$] | 343.45 | 515.74 |
| $T$ [K] | 293(2) | 293(2) |
| crystal system | monoclinic | monoclinic |
| space group | $P2_1/c$ | $C2/c$ |
| $a$ [Å] | 7.466(4) | 29.915(17) |
| $b$ [Å] | 3.953(2) | 7.819 (9) |
| $c$ [Å] | 47.346(14) | 21.266 (20) |
| $\alpha$ [°] | 90 | 90 |
| $\beta$ [°] | 97.85(4) | 124.40(13) |
| $\gamma$ [°] | 90 | 90 |
| $V$ [Å$^3$] | 1384.2(11) | 4104.9(9) |
| $Z$ | 4 | 8 |
| $\rho_{calcd}$ [g cm$^{-3}$] | 1.648 | 1.68 |
| $\mu$ [mm$^{-1}$] | 0.689 | 0.884 |
| goodness-of-fit on $F^2$ | 0.916 | 1.001 |
| final $R1/wR2$ [$I > 2\sigma(I)$] | 0.075/0.0969 | 0.0537/0.0887 |
| $R1/wR2$ (all data) | 0.2398/0.1341 | 0.1299/0.1068 |

**EPR measurements**: EPR spectra were recorded on a Bruker 300 spectrometer (X-band). Electrochemical oxidations were carried out in situ in the EPR cavity by using a two-electrode cell; solutions in THF or $CH_2Cl_2$ ($10^{-6}$ M) were carefully dried and degassed, ammonium hexafluorophosphate (0.1 M) was used as supporting electrolyte. Sample tubes for the study of chemical oxidation products were prepared inside a glove-box.

**Theoretical calculations**: The optimized geometries were obtained with the Gaussian 03[33] package at the DFT level of theory. The B3LYP functional[34] with the 6-31+G* basis set was used. Vibrations frequency calculations performed on the optimized structures at the same level of theory yielded only positive values. Time-dependent DFT calculations were performed at the B3LYP/6-31G* level on the equilibrium geometry corresponding to the conformation found in the crystal structure. Hyperfine coupling constants were calculated at the DFT/B3LYP/aug-cc-pPVDZ level.

## Acknowledgements

This work was supported by the Ministry of Education and Research (grant to F.R.), the CNRS (France) and the Swiss National Science Foundation (Switzerland). Financial support from the French Ministry of Foreign Affairs through a Germaine de Staël 2006–2007 (PHC 10613RJ) project is also acknowledged.

[1] a) J. L. Segura, N. Martin, *Angew. Chem.* **2001**, *113*, 1416; *Angew. Chem. Int. Ed.* **2001**, *40*, 1372; b) J.-L. Yamada, *TTF Chemistry: Fundamentals and Applications of Tetrathiafulvalene*, Springer, Heidelberg, **2004**.
[2] T. Ishiguro, K. Yamaji, G. Saito, *Organic Superconductors*, Springer, Heidelberg, **1998**.
[3] a) M. R. Bryce, *Adv. Mater.* **1999**, *11*, 11; b) M. Bendikov, F. Wudl, D. F. Perepichka, *Chem. Rev.* **2004**, *104*, 4891.
[4] A. Aviram, M. A. Ratner, *Chem. Phys. Lett.* **1974**, *29*, 277.
[5] a) C. Jia, S.-X. Liu, C. Tanner, C. Leiggener, A. Neels, L. Sanguinet, E. Levillain, S. Leutwyler, A. Hauser, S. Decurtins, *Chem. Eur. J.* **2007**, *13*, 3804; b) C. Goze, C. Leiggener, S.-X. Liu, L. Sanguinet, E. Levillain, A. Hauser, S. Decurtins, *ChemPhysChem* **2007**, *8*, 1504.

  

[6] N. Gautier, F. Dumur, V. Lloveras, J. Vidal-Gancedo, J. Veciana, C. Rovira, P. Hudhomme, *Angew. Chem.* **2003**, *115*, 2871; *Angew. Chem. Int. Ed.* **2003**, *42*, 2765.
[7] Naraso, J. Nishida, M. Tomura, Y. Yamashita, *Synth. Met.* **2005**, *153*, 389.
[8] C. Loosli, C. Jia, S.-X. Liu, M. Haas, M. Dias, E. Levillain, A. Neels, G. Labat, A. Hauser, S. Decurtins, *J. Org. Chem.* **2005**, *70*, 4988.
[9] D. F. Perepichka, M. R. Bryce, C. Pearson, M. C. Petty, E. J. L. McInnes, J. P. Zhao, *Angew. Chem.* **2003**, *115*, 4784; *Angew. Chem. Int. Ed.* **2003**, *42*, 4636.
[10] a) D. F. Perepichka, M. R. Bryce, A. S. Batsanov, J. A. K. Howard, A. O. Cuello, M. Gray, V. M. Rotello, *J. Org. Chem.* **2001**, *66*, 4517; b) J. Wu, S.-X. Liu, A. Neels, F. Le Derf, M. Sallé, S. Decurtins, *Tetrahedron* **2007**, *63*, 11282.
[11] D. M. Guldi, F. Giacalone, G. de la Torre, J. L. Segura, N. Martin, *Chem. Eur. J.* **2005**, *11*, 7199.
[12] M. Á. Herranz, N. Martin, S. Campidelli, M. Prato, G. Brehm, D. M. Guldi, *Angew. Chem.* **2006**, *118*, 4590; *Angew. Chem. Int. Ed.* **2006**, *45*, 4478.
[13] G. Ho, J. R. Heath, M. Kondratenko, D. F. Perepichka, K. Arseneault, M. Pézolet, M. R. Bryce, *Chem. Eur. J.* **2005**, *11*, 2914.
[14] T. Murata, Y. Morita, Y. Yakiyama, Y. Nishimura, T. Ise, D. Shiomi, K. Sato, T. Takui, K. Nakasuji, *Chem. Commun.* **2007**, 4009.
[15] L. M. Goldenberg, J. Y. Becker, O. P.-T. Levi, V. Y. Khodorkovsky, L. M. Shapiro, M. R. Bryce, J. P. Cresswell, M. C. Petty, *J. Mater. Chem.* **1997**, *7*, 901.
[16] R. Andreu, I. Malfant, P. G. Lacroix, P. Cassoux, *Eur. J. Org. Chem.* **2000**, 737.
[17] Y.-P. Zhao, L.-Z. Wu, G. Si, Y. Liu, H. Xue, L.-P. Zhang, C.-H. Tung, *J. Org. Chem.* **2007**, *72*, 3632.
[18] C. Goze, S.-X. Liu, C. Leiggener, L. Sanguinet, E. Levillain, A. Hauser, S. Decurtins, *Tetrahedron* **2008**, *64*, 1345.
[19] a) O. P.-T. Levi, J. Y. Becker, A. Ellern, V. Khodorkovsky, *Tetrahedron Lett.* **2001**, *42*, 1571; b) Q.-Y. Zhu, Y. Liu, W. Lu, Y. Zhang, G.-Q. Bian, G.-Y. Niu, J. Dai, *Inorg. Chem.* **2007**, *46*, 10065.
[20] S. Nishida, Y. Morita, K. Fukui, K. Sato, D. Shiomi, T. Takui, K. Nakasuji, *Angew. Chem.* **2005**, *117*, 7443; *Angew. Chem. Int. Ed.* **2005**, *44*, 7277.
[21] S. Bouguessa, A. K. Gouasmia, S. Golhen, L. Ouahab, J. M. Fabre, *Tetrahedron Lett.* **2003**, *44*, 9275.
[22] a) J. Pang, Y. Tao, S. Freiberg, X.-P. Yang, M. D'Iorio, S. Wang, *J. Mater. Chem.* **2002**, *12*, 206; b) T. Murase, M. Fujita, *J. Org. Chem.* **2005**, *70*, 9269.
[23] G. Cooke, A. K. Powell, S. L. Heath, *Synthesis* **1995**, 1411.
[24] Experimental details and characterization of compounds, X-ray data, UV-Vis spectra, cyclic voltammetry details, theoretical calculations details are provided in the Supporting Information. CCDC 670739 (**1**)and 670740 (**2**) contain the supplementary crystallographic data for this paper. These data can be obtained free of charge from The Cambridge Crystallographic Data Centre via www.ccdc.cam.ac.uk/data_request/cif.
[25] a) M. Mas-Torrent, M. Durkut, P. Hadley, X. Ribas, C. Rovira, *J. Am. Chem. Soc.* **2004**, *126*, 984; b) M. Mas-Torrent, C. Rovira, *J. Mater. Chem.* **2006**, *16*, 433.
[26] M. Behl, R. Zentel, *Macromol. Chem. Phys.* **2004**, *205*, 1633.
[27] a) M. Iyoda, M. Fukuda, M. Yoshida, S. Sasaki, *Chem. Lett.* **1994**, 2369; b) M. Iyoda, M. Fukuda, S. Sasaki, M. Yoshida, *Synth. Met.* **1995**, *70*, 1171.
[28] H. Mizouchi, A. Ikawa, H. Fukutome, *J. Am. Chem. Soc.* **1995**, *117*, 3260.
[29] J. Yamauchi, T. Aoyama, K. Kanemoto, S. Sasaki, M. Iyoda, *J. Phys. Org. Chem.* **2000**, *13*, 197.
[30] R. M. Dupeyre, H. Lemaire, A. Rassat, *J. Am. Chem. Soc.* **1965**, *87*, 3771.
[31] R. Ziessel, G. Ulrich, R. C. Lawson, L. Echegoyen, *J. Mater. Chem.* **1999**, *9*, 1435.
[32] G. M. Sheldrick, Programs for the Refinement of Crystal Structures, University of Göttingen, Göttingen (Germany), **1996**.
[33] Gaussian 03, Revision B.03, M. J. Frisch, G. W. Trucks, H. B. Schlegel, G. E. Scuseria, M. A. Robb, J. R. Cheeseman, J. A. Montgomery, Jr., T. Vreven, K. N. Kudin, J. C. Burant, J. M. Millam, S. S. Iyengar, J. Tomasi, V. Barone, B. Mennucci, M. Cossi, G. Scalmani, N. Rega, G. A. Petersson, H. Nakatsuji, M. Hada, M. Ehara, K. Toyota, R. Fukuda, J. Hasegawa, M. Ishida, T. Nakajima, Y. Honda, O. Kitao, H. Nakai, M. Klene, X. Li, J. E. Knox, H. P. Hratchian, J. B. Cross, V. Bakken, C. Adamo, J. Jaramillo, R. Gomperts, R. E. Stratmann, O. Yazyev, A. J. Austin, R. Cammi, C. Pomelli, J. W. Ochterski, P. Y. Ayala, K. Morokuma, G. A. Voth, P. Salvador, J. J. Dannenberg, V. G. Zakrzewski, S. Dapprich, A. D. Daniels, M. C. Strain, O. Farkas, D. K. Malick, A. D. Rabuck, K. Raghavachari, J. B. Foresman, J. V. Ortiz, Q. Cui, A. G. Baboul, S. Clifford, J. Cioslowski, B. B. Stefanov, G. Liu, A. Liashenko, P. Piskorz, I. Komaromi, R. L. Martin, D. J. Fox, T. Keith, M. A. Al-Laham, C. Y. Peng, A. Nanayakkara, M. Challacombe, P. M. W. Gill, B. Johnson, W. Chen, M. W. Wong, C. Gonzalez, J. A. Pople, Gaussian, Inc., Wallingford CT, **2004**.
[34] a) C. Lee, W. Yang, R. G. Parr, *Phys. Rev. B* **1988**, *37*, 785; b) A. D. Becke, *J. Chem. Phys.* **1993**, *98*, 5648.

Received: September 8, 2008
Published online: November 19, 2008

  